

Supporting Information

Impact of Molecular Solvophobicity vs Solvophilicity on Device Performances of Dimeric Perylene Diimide Based Solution-Processed Non-Fullerene Organic Solar Cells

Zhenhuan Lu,[†] Xin Zhang,[†] Chuanlang Zhan,* Bo Jiang, Xinliang Zhang, Lili Chen, and Jiannian Yao*

Beijing National Laboratory for Molecular Sciences, CAS Key Laboratory of Photochemistry, Institute of Chemistry, Chinese Academy of Sciences, Beijing 100080, P. R. China. Tel/Fax: +86-10-82616517/82617312, E-mail: (C.Z.) clzhan@iccas.ac.cn, (J.Y.) jnyao@iccas.ac.cn.

Contents

1. Experimental section	2
2. Synthesis	4
3. Supporting figures.....	7
Fig. S1	7
Fig. S2	8
Fig. S3	8
Fig. S4	8
Fig. S5	9
Fig. S6	9
Fig. S7	9
Fig. S8	10
Fig. S9	11
Fig. S10	12
4. Supporting tables.....	15
References.....	15

1. Experimental section

1.1. Materials

All reagents and chemicals were purchased from commercial sources (TCI, Acros, Sigma, or Alfa) and used without further purification except statements. Solvents (toluene and tetrahydrofuran) were distilled by standard procedures before used for organic synthesis.

1.2. Instruments and measurements

^1H NMR and ^{13}C NMR spectra were recorded by a Bruker DMX-400 spectrometer with CDCl_3 as a solvent and tetramethylsilane as an internal reference. MALDI-TOF mass spectra were recorded by a Bruker BIFLEXIII. Absorption spectra were taken on a Hitachi U-3010 UV-vis spectrophotometer. The pristine films on quartz plate used for the UV measurements were prepared by spin-coating a 1 mg/mL chloroform solution of the samples. The blending films used for absorption spectrum measurements were prepared on silica substrate under the same conditions (e.g. donor/acceptor ratio, spin-coating speed, solvent) to the preparation of photovoltaic devices that afford the best performances. The electrochemical cyclic voltammetry (CV) was performed using a Zahner IM6e electrochemical workstation in a 0.1 mol/L tetrabutylammonium hexafluorophosphate (Bu_4NPF_6) dichloromethane (DCM) solution with a scan speed at 0.1 V/s. A Pt wire and Ag/AgCl were used as the counter and reference electrodes, respectively. The concentration of **Bis-PDI-T**, **Bis-PDI-T-EG** and **Bis-PDI-T-di-EG** is adjusted as 1×10^{-4} mol/L in chromatographic pure DCM solution) for the measurements cyclic voltammetry (CV). Thermogravimetric analysis (TGA) was performed on a Perkin-Elmer TGA-7 at a heating rate of 10 °C/min under nitrogen flow. Atom force microscopy (AFM) was investigated by Brucker Multimode 8 using tapping-mode with a scan speed of 1Hz. X-ray diffraction (XRD) samples of pristine polymer films or blending films were prepared by spin-casting of solutions on silica slides. The XRD pattern was recorded by a Rigaku D/max-2500 diffractometer operated at 40 kV voltage and a 200 mA current with Cu K α radiation. The differential scanning calorimetry (DSC) was recorded by Mettler Toledo-822e at a heating rate of 10 °C/min.

1.3. Quantum chemical calculations

Computational details are presented as follows: Density functional theory calculations were performed with the Gaussian 09 program,¹ using the B3LYP functional.² All-electron double- ξ valence basis sets with polarization functions³ 6-31G* were used for all atoms. Geometry optimizations were performed with full relaxation of all atoms in gas phase without solvent effects. Vibrational frequency calculations were performed to check that the stable structures had no imaginary frequency. Charge distribution of the molecules was calculated by Mulliken population analysis.

1.4. Fabrication and characterizations of OSCs

OSCs with a typical configuration of ITO/PEDOT: PSS/ **P3HT:PDI dimer** /Ca/Al was fabricated as follows. The ITO glass was pre-cleaned with deionized water, CMOS grade acetone and isopropanol in turn for 15 min. The organic residues were further removed by treating with UV-ozone for 1 h. Then the ITO glass was modified by spin-coating PEDOT: PSS (poly(3,4-ethylenedioxythiophene)-poly(styrenesulfonate) layer, 30 nm) on it. After the ITO glasses were dried in oven at 150 °C for 15 min, the

active layer was spin-coated on the ITO/PEDOT:PSS using a blend solution of **P3HT** and **PDI dimer** (10 mg/mL in CHCl₃ for **Bis-PDI-T**, 40 mg/mL in o-dichlorobenzene (ODCB) for **Bis-PDI-T-EG** and **Bis-PDI-T-di-EG**, variants with donor/acceptor weight ratio, respectively). Ca (20 nm) and Al (80 nm) electrode was then subsequently thermally evaporated on the active layer under the vacuum of 1×10⁻⁶ Torr. The active area of the device was 0.06 cm², and the thickness of the active films were ~100 nm. The devices were characterized in nitrogen atmosphere under the illumination of simulated AM 1.5 G, 100 mW/cm² using a xenon-lamp-based solar simulator. The current-voltage (*I-V*) measurement of the devices was conducted on a computer-controlled Keithley 2400 Source Measure Unit. The EQE measurements of the encapsulated devices were performed in air (PV Measurements Inc., Model QEX7).

1.5. Tests of the charge carrier mobilities ^[4]

1.5.1 Hole mobilities measurement

The devices were fabricated with a configuration of ITO/PEDOT : PSS (30nm) / P3HT:PDI dimer(220-260nm) /Au(600nm). The active layers were spin-coated under the conditions that afford the best photovoltaic results. The following equation was applied to estimate the hole mobilities:

$$J=9/8\epsilon\epsilon_0\mu_h V^2/L^3 \exp[0.89(V/E_0L)^{0.5}] \quad (1)$$

where ϵ is the average dielectric constant of the blended film, ϵ_0 the permittivity of the vacuum, μ_0 the zero-field mobility, E_0 the characteristic field, J the current density, L the thickness of the films, and $V = V_{\text{appl}} - V_{\text{bi}}$; V_{appl} the applied potential, and V_{bi} the built-in potential which results from the difference in the work function of the anode and the cathode (in this device structure, $V_{\text{bi}} = 0.2$ V). The results are plotted as $\ln(JL^3/V^2)$ vs $(V/L)^{0.5}$, as shown in Figure S8. The hole mobility of the blending films was deduced from the intercept value of $\ln(9\epsilon\epsilon_0\mu_0/8)$.

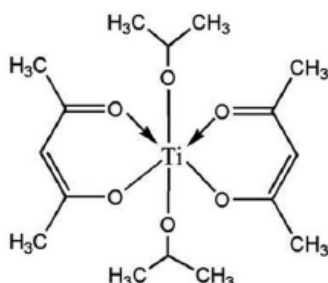
1.5.2 Electron mobilities measurement

The devices were fabricated with a configuration of ITO/titanium (diisopropoxide bis(2,4-pentanedionate)^{4c} (TIPD, 20nm) / P3HT:PDI dimer(120-150nm) /Al(1000nm). Since the HOMO and LUMO energy levels of the TIPD were -3.91 eV and -6.0 eV, it can be used to fabricate the electron-only SCLC device. The TIPD buffer layer was prepared by spin-coating (3000 rpm) a 3.5 wt % TIPD isopropanol solution on the pre-cleaned ITO substrate and then baked at 150 °C for 10 min. Subsequently, the blended films were prepared using the same condition as the preparation of the best OSC device. Finally, a 1000 nm Al layer was thermally deposited on the top of the blended films in vacuum. Electron mobilities were extracted by fitting the current density–voltage curves using the Mott–Gurney relationship (space charge limited current) as follows:

$$J=9/8\epsilon\epsilon_0\mu_e V^2/L^3 \exp[0.89(V/E_0L)^{0.5}] \quad (1)$$

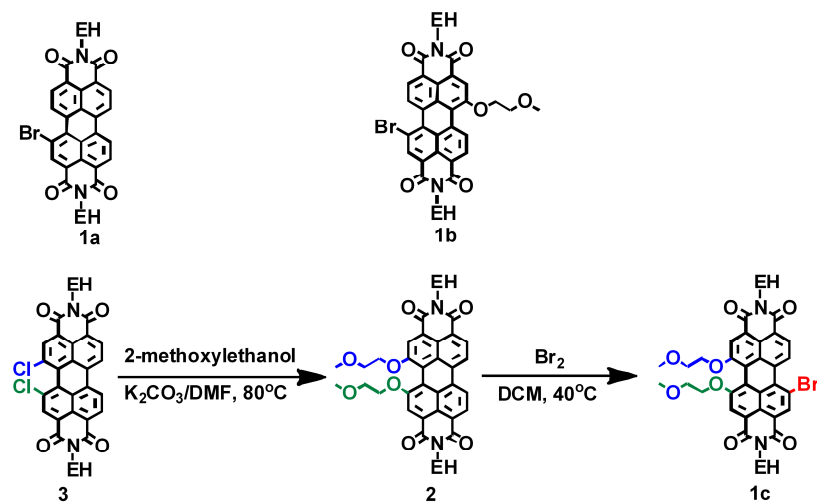
where ϵ is the average dielectric constant of the blended film, ϵ_0 the permittivity of the vacuum, μ_0 the zero-field mobility, E_0 the characteristic field, J the current density, L the thickness of the films, and $V = V_{\text{appl}} - V_{\text{bi}}$; V_{appl} the applied potential, and V_{bi} the built-in potential which results from the difference in the work function of the anode and the cathode (in this device structure, $V_{\text{bi}} = 0.2$ V). The results are plotted as $\ln(JL^3/V^2)$ vs $(V/L)^{0.5}$, as shown in Figure S9. The electron mobility of the blending films was deduced from the intercept value of $\ln(9\epsilon\epsilon_0\mu_0/8)$.

Following shows the chemical structure of TIPD.



TIPD

2. Synthesis



2.1. Synthesis of compounds 1a, 1b, 3

1a, 1b and 3 were synthesized according to the literature methods, respectively.^[5-7]

2.2. Synthesis of compound 2

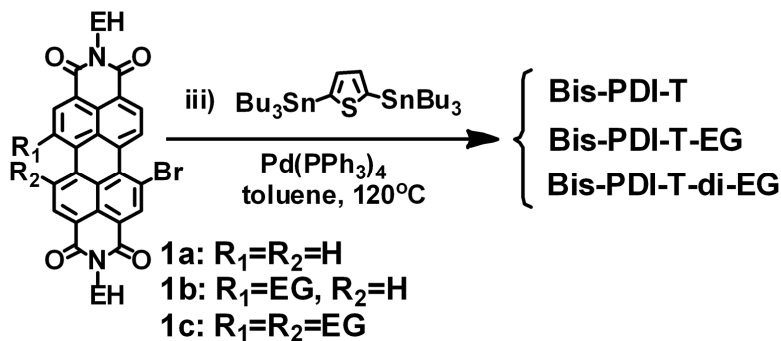
A mixture of 3 (136.4 mg, 0.2 mmol), 2-methoxyethanol (76.1 mg, 1.0 mmol) and potassium carbonate (K_2CO_3 , 140 mg, 1.0 mmol) in 10 mL dimethylformamide (DMF) was heated at 80°C. The reaction was monitored by using TLC. Then, the reaction mixture was poured into 30 mL water and the red solid was re-dissolved in 20 mL DCM and washed with 1N hydrochloric acid and then water each for 3 times. Then, the DCM layer was dried over Na_2SO_4 . After removal of DCM, the residue was purified by column chromatography on silica gel (DCM/EtOH, 100:1-50:1 v/v) to afford 2 as a dark-red solid (15.3 mg, 0.02 mmol, yield = 20%). 1H -NMR ($CDCl_3$, 400MHz) δ ppm: 8.46 (d, J = 8.00 Hz, 2H), 8.41 (s, 2H), 8.37 (d, J = 8.00 Hz, 2H), 4.50 (m, 4H), 4.15 (m, 4H), 3.79 (m, 4H), 3.39 (s, 6H), 1.96 (m, 2H), 1.40 (m, 8H), 1.33 (m, 8H), 0.95 (m, 6H), 0.90 (m, 6H). ^{13}C -NMR (100 MHz, $CDCl_3$) δ ppm: 163.98, 163.89, 156.19, 133.09, 128.55, 128.21, 123.41, 122.74, 122.38, 121.66, 119.78, 117.97, 71.33, 68.80, 59.35, 44.37, 38.10, 30.93, 28.89, 24.20, 23.21, 14.25, 10.78. MS (MALDI-TOF): m/z = 763.5 [M+H]⁺.

2.3. Synthesis of compound 1c

A mixture of 2 (76.3 mg, 0.1 mmol) was dissolved into 20 mL of DCM, to which 1 mL bromine was dropwise added. The mixture was heated at 50°C. The reaction was monitored by using TLC. The excess of bromine was removed by flow of N₂, and the solvent was removed under vacuum. It was purified by column chromatography on silica gel (DCM/EtOH, 50:1 v/v) to afford compound 1c as a dark-red solid

(60.3 mg, 0.095 mmol, yield = 95%). $^1\text{H-NMR}$ (CDCl_3 , 400MHz) δ ppm: 9.38 (d, J = 8.00 Hz, 1H), 8.78 (s, 1H), 8.55 (d, J = 8.00 Hz, 1H), 8.43 (s, 2H), 4.54 (m, 2H), 4.44 (m, 2H), 4.17 (m, 4H), 3.75 (m, 4H), 3.36 (s, 6H), 1.96 (m, 2H), 1.42 (m, 8H), 1.33 (m, 8H), 0.96 (m, 6H), 0.90 (m, 6H). $^{13}\text{C-NMR}$ (100 MHz, CDCl_3) δ ppm: 164.21, 163.87, 163.84, 163.01, 156.50, 156.46, 135.39, 132.16, 131.99, 130.95, 129.98, 127.44, 127.27, 122.92, 122.89, 122.52, 122.18, 121.93, 121.73, 120.34, 119.63, 119.07, 117.55, 117.31, 71.17, 68.91, 59.32, 59.28, 44.51, 44.41, 38.14, 38.11, 30.90, 28.88, 24.20, 23.21, 23.18, 14.25, 10.78, 10.77. MS (MALDI-TOF): m/z = 842.9 [M+H] $^+$.

2.4. Synthesis of Bis-PDI-T, Bis-PDI-T-EG and Bis-PDI-T-di-EG



A mixture of **1a**, **1b** or **1c** (0.22 mmol) and 2, 5-bis(tributylstannyl) thiophene (97%, 0.1mmol) was dissolved in dry toluene (10 mL). Catalytic amounts of $\text{Pd}[\text{P}(\text{C}_6\text{H}_5)_3]_4$ was added and the reaction mixture was stirred at 120 °C for 36 hours. The mixture was extracted with dichloromethane (DCM), washed with water. Then, DCM layer was dried over Na_2SO_4 . After removal of DCM, the residue was applied to chromatography to afford the desired products of **Bis-PDI-T**, **Bis-PDI-T-EG**, or **Bis-PDI-T-di-EG**.

For **Bis-PDI-T**: using CH_2Cl_2 /ethanol (100:1) as eluents to afford the final product as a black solid (**119.3 mg, 0.09 mmol, yield = 82%**). $^1\text{H-NMR}$ (400MHz, CDCl_3) δ ppm: 8.76-8.53 (m, 12H), 8.39 (m, 2H), 7.48 (s, 2H), 4.24-3.98 (m, 8H), 2.05-1.84 (m, 2H), 1.49-1.19 (m, 32H), 1.04-0.79 (m, 24H). Since the solubility of **Bis-PDI-T** is very low, it is impossible to perform $^{13}\text{C-NMR}$ characterization. MS (MALDI-TOF): m/z = 1309.8 [M+H] $^+$. Elemental analysis: calcd (%) for $\text{C}_{84}\text{H}_{84}\text{N}_4\text{O}_8\text{S}\cdot 2\text{H}_2\text{O}$: C 74.97, H 6.59, N 4.16, S 2.45; found C 74.93, H 6.56, N 4.20, S 2.42.

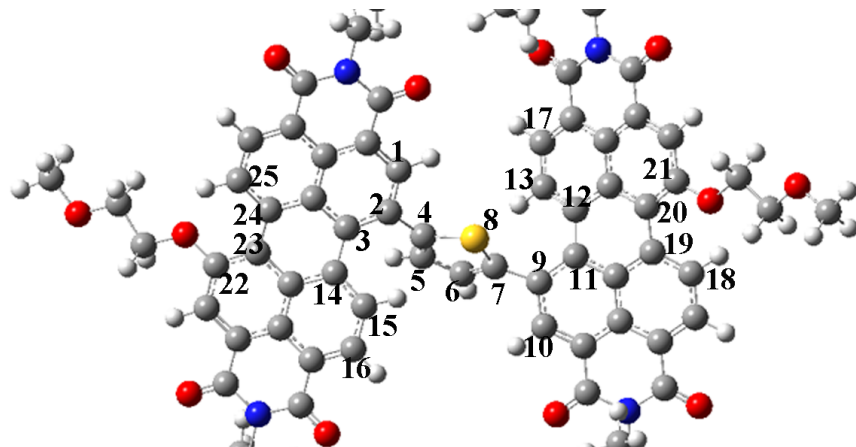
For **Bis-PDI-T-EG**: using CH_2Cl_2 /methanol (20:1) as eluents to afford the final products as black solid (**116.6 mg, 0.08 mmol, yield = 80%**). $^1\text{H-NMR}$ (400MHz, CDCl_3) δ ppm: 9.54 (d, J = 8.08 Hz, 2H), 8.66 (s, 2H), 8.66 (d, J = 7.60 Hz, 2H), 8.54 (d, 6.92 Hz, 2H), 8.36 (s, 2H), 8.27 (d, J = 8.00 Hz, 2H), 7.46 (s, 2H), 4.61 (s, 4H), 4.25-4.02 (m, 8H), 3.98 (s, 4H), 3.59 (s, 6H), 1.97 (s, 2H), 1.88 (s, 2H), 1.41-1.33 (m, 32H), 0.98-0.90 (m, 12H), 0.90-0.81 (m, 12H). $^{13}\text{C-NMR}$ (100 MHz, CDCl_3) δ ppm: 163.9, 163.5, 163.3, 157.0, 146.9, 135.2, 134.0, 131.5, 131.3, 130.5, 129.2, 128.8, 128.5, 127.7, 127.4, 123.8, 123.4, 122.4, 121.7, 121.4, 120.4, 117.6, 70.9, 69.4, 59.5, 44.5, 38.1, 38.0, 31.0, 28.9, 28.8, 24.3, 24.1, 23.2, 14.3, 14.2, 10.8. Elemental Analysis for $\text{C}_{90}\text{H}_{96}\text{N}_4\text{O}_{12}\text{S}\cdot 3\text{H}_2\text{O}$: Calcd C, 71.50; H, 6.80; N, 3.71; S, 2.12; Found C, 71.45; H, 6.57; N, 3.88; S, 2.14. TOF MS: m/z = 1457.1 [M+H] $^+$.

For **Bis-PDI-T-di-EG**: using CH_2Cl_2 /ethanol (75:1-50:1) as eluents to afford the final products as a black solid (**133.2 mg, 0.083 mmol, yield = 83%**). $^1\text{H-NMR}$ (400MHz, CDCl_3) δ ppm: 8.68-8.50 (m, 2H), 8.49-8.42 (s, 2H), 8.42-8.27 (m, 4H), 8.26-8.18 (m, 2H), 7.49-7.37 (s, 2H), 4.65-4.35 (m, 8H), 4.27-3.95 (m,

8H), 3.89-3.62 (m, 8H), 3.36 (s, 12H), 2.10-1.81 (m, 4H), 1.49-1.18 (m, 32H), 1.03-0.76 (m, 24H). ^{13}C -NMR (100 MHz, CDCl_3) δ ppm: 164.38, 164.32, 164.10, 156.92, 156.72, 146.79, 133.66, 133.16, 132.66, 132.40, 132.30, 130.82, 130.63, 129.16, 128.87, 127.26, 123.56, 123.16, 123.07, 122.95, 122.29, 121.88, 121.73, 120.89, 119.78, 119.49, 118.25, 117.91, 71.35, 71.33, 69.09, 59.44, 59.42, 44.62, 44.50, 38.28, 38.21, 31.06, 30.98, 29.02, 24.35, 24.22, 23.31, 14.37, 10.91. MS (MALDI-TOF): m/z = 1606.2 [M+H]⁺. Elemental analysis: calcd (%) for $\text{C}_{96}\text{H}_{108}\text{N}_4\text{O}_{16}\text{S}\cdot 3\text{H}_2\text{O}$: C 69.46, H 6.92, N 3.38, S 1.93; found C 69.42, H 6.89, N 3.42, S 1.96.

3. Supporting figures

Figure S1. The optimal conformation of Bis-PDI-T-EG and the dihedral angles of Bis-PDI-T, Bis-PDI-T-EG and Bis-PDI-T-di-EG shown in the following table.



Bis-PDI-T:

Atom Number	1-2-4-5	1-2-4-8	3-2-4-5	3-2-4-8
$\theta (\circ)$	-124.55	49.71	51.02	-134.71
Atom Number	10-9-7-8	10-9-7-6	11-9-7-8	11-9-7-6
$\theta (\circ)$	117.26	-56.69	-58.51	127.54
	9-11-12-13	18-19-20-21	2-3-14-15	22-23-24-25
$\theta (\circ)$	-18.69	-10.22	19.49	10.07
	15-16-13-17	1-2-9-10		
$\theta (\circ)$	-22.88	161.65		

Bis-PDI-T-EG:

Atom Number	1-2-4-5	1-2-4-8	3-2-4-5	3-2-4-8
$\theta (\circ)$	-125.48	49.58	50.05	-134.88
Atom Number	10-9-7-8	10-9-7-6	11-9-7-8	11-9-7-6
$\theta (\circ)$	120.12	-53.44	-55.84	130.59
	9-11-12-13	18-19-20-21	2-3-14-15	22-23-24-25
$\theta (\circ)$	-20.64	-15.80	21.01	15.24
	15-16-13-17	1-2-9-10		
$\theta (\circ)$	-19.10	164.13		

Bis-PDI-T-di-EG:

Atom Number	1-2-4-5	1-2-4-8	3-2-4-5	3-2-4-8
$\theta (\circ)$	-127.86	47.18	48.01	-136.93
Atom Number	10-9-7-8	10-9-7-6	11-9-7-8	11-9-7-6
$\theta (\circ)$	118.71	-55.29	-58.01	127.99
	9-11-12-13	18-19-20-21	2-3-14-15	22-23-24-25
$\theta (\circ)$	-20.74	-32.63	22.10	32.37
	15-16-13-17	1-2-9-10		
$\theta (\circ)$	-24.47	160.26		

Noted: $\theta (\circ)$ is the dihedral angle along the selected atoms.

Figure S2. (a) TGA and (b) DSC curves of the three PDI dimers.

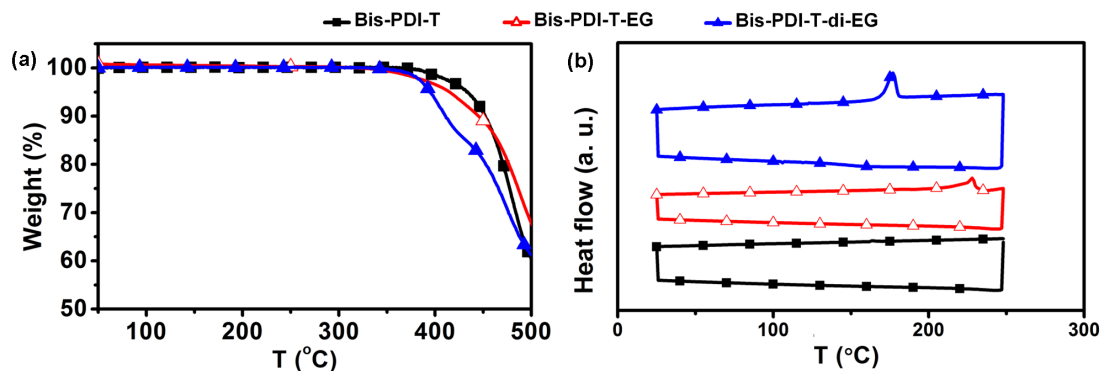


Figure S3. (a) Photoluminescence (PL) spectra of the films of P3HT ($\lambda_{\text{ex}}=522\text{nm}$), **Bis-PDI-T** ($\lambda_{\text{ex}}=550\text{nm}$), **Bis-PDI-T-EG** ($\lambda_{\text{ex}}=550\text{nm}$), **Bis-PDI-T-di-EG** ($\lambda_{\text{ex}}=600\text{nm}$) and the blend of P3HT/**Bis-PDI-T-EG** ($\lambda_{\text{ex}}=522\text{nm}$). The PL of the P3HT/PDI (1:1, w/w) dimers blending films was completely quenched, and we only show P3HT/**Bis-PDI-T-EG** as a representative case. (b) Photobleaching kinetics of the PDI dimers films under continuous illumination with a 4.0 mW light at $\lambda_{\text{ex}}=550\text{ nm}$ (**Bis-PDI-T** and **Bis-PDI-T-EG**) and $\lambda_{\text{ex}}=600\text{nm}$ (**Bis-PDI-T-di-EG**).

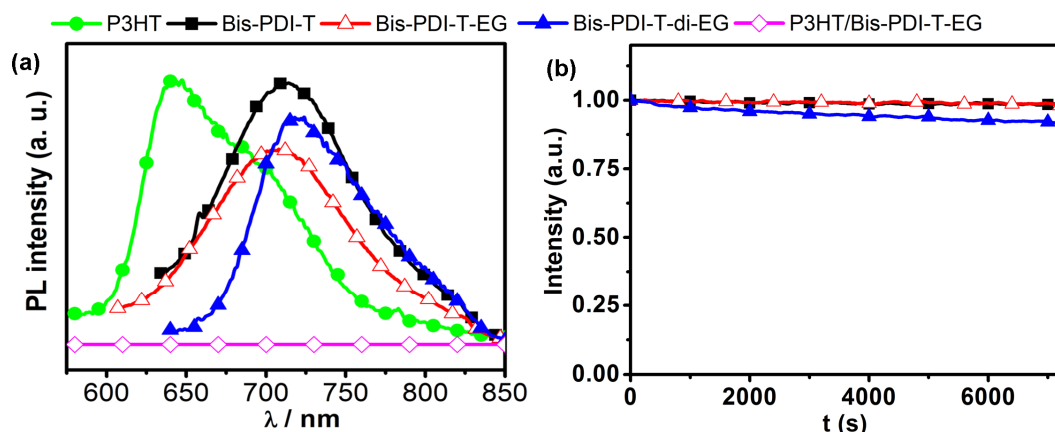


Figure S4. Cyclic voltammogram of P3HT in a 0.1 mol L^{-1} $\text{Bu}_4\text{NPF}_6/\text{CH}_2\text{Cl}_2$ solution with a scan rate of 100 mV s^{-1} and using Ag/AgCl as the reference electrode.

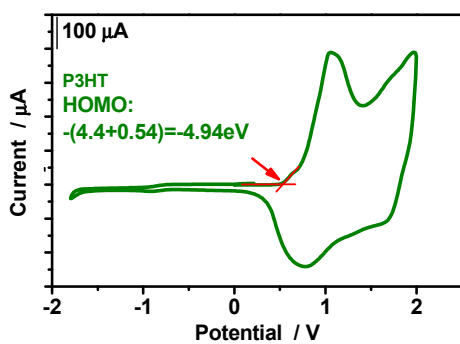


Figure S5. The $J-V$ curves of the P3HT only OSCs device.

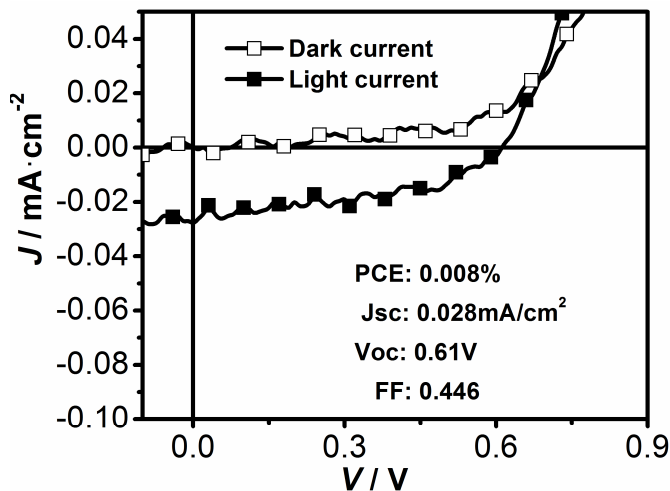


Figure S6. Optical images of the 1:1 blended P3HT:**Bis-PDI-T** after using 3% of Cl-Naph as the co-solvent of *o*-DCB.

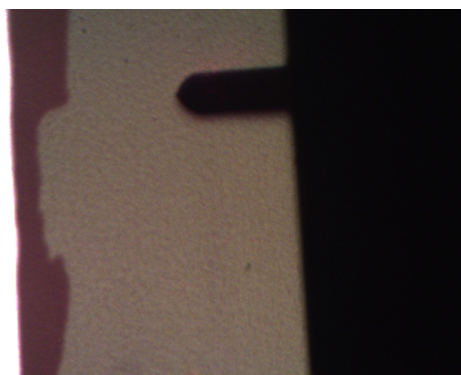
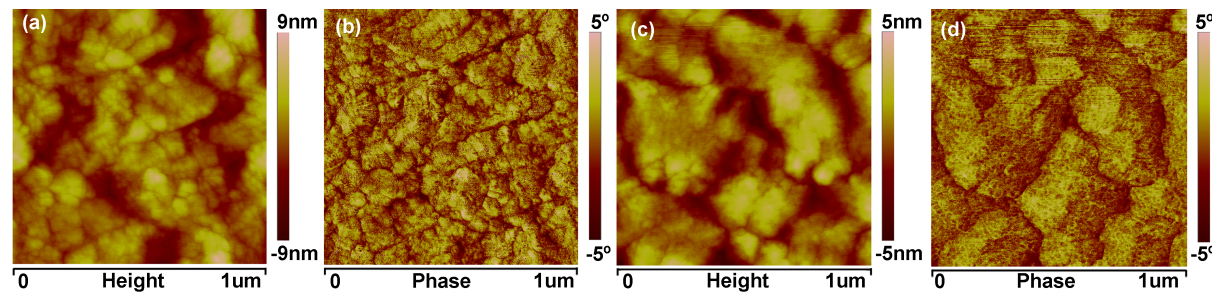


Figure S7. The AFM height (a, c) and phase (b, d) images of the blended films of **Bis-PDI-T-EG** and **P3HT** with a D/A weight ratio of 2/1 (a, b) and 1/2 (c, d), respectively. These experiments were conducted to determine which phase was mainly contributed from P3HT and which one was from the PDI dimer.



From the height and phase images of the 2/1 and 1/2 blended D/A films, one can see that the bright phases become smaller as the weight percentage of **P3HT** decreases, indicating that the bright phases are mainly contributed from the electron-donor of **P3HT**. Accordingly, the dark phases are mainly from the PDI dimer of **Bis-PDI-T-EG**, the electron-acceptor.

Figure S8. The $J-V$ curves extracted from the SCLC data of the blended films of P3HT/PDI dimer: P3HT/**Bis-PDI-T** with 0% (a) and 3% (b) of Cl-Naph; P3HT/**Bis-PDI-T-EG** with 0% (c) and 8% (d) of Cl-Naph; P3HT/**Bis-PDI-T-di-EG** with 0% (e) and 1.75% (f) of Cl-Naph. The hole mobilities (μ_h) are listed in Table 3 in the text.

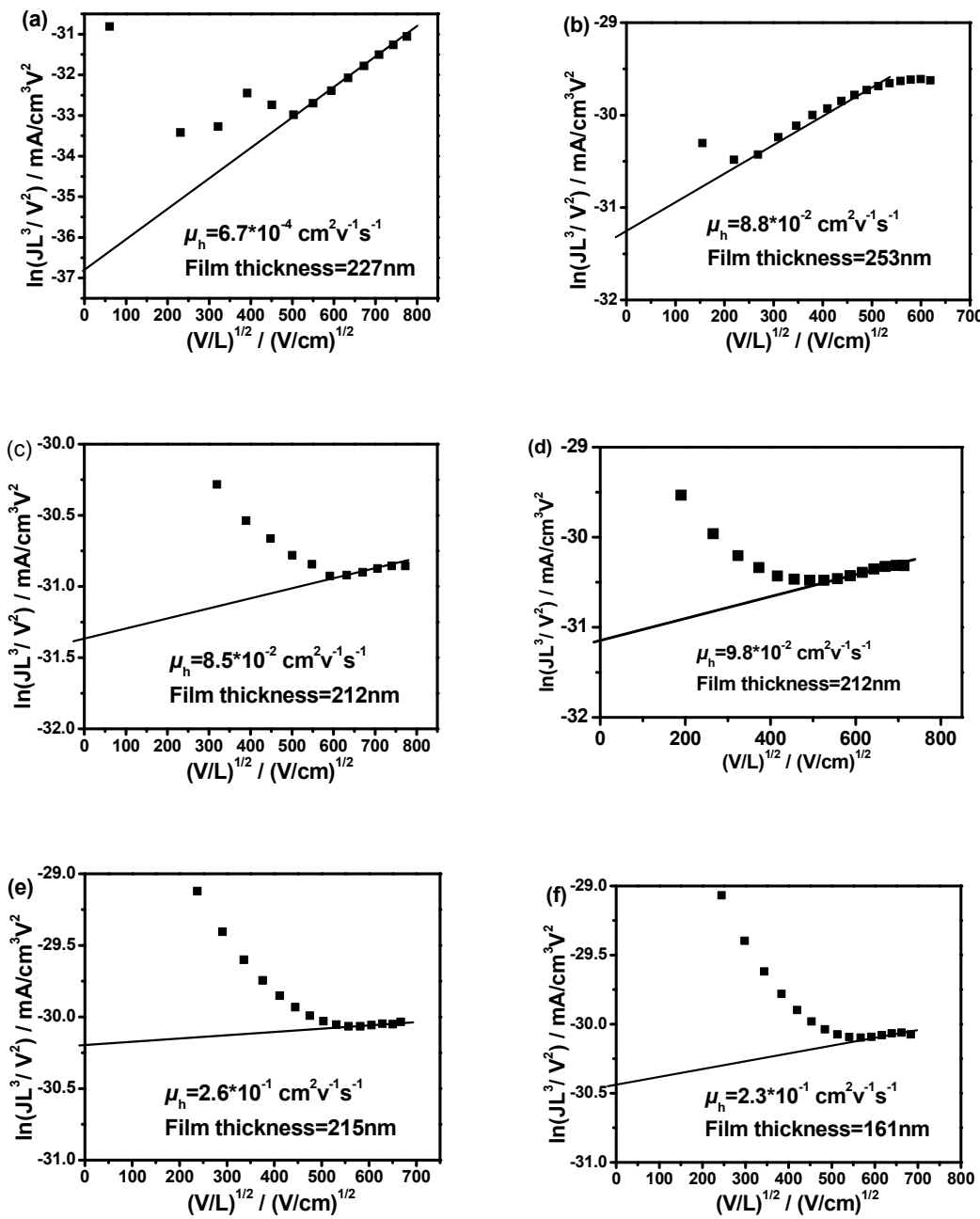


Figure S9. The $J-V$ curves extracted from the SCLC data of the blended films of P3HT/PDI dimer: P3HT/**Bis-PDI-T** with 0% (a) and 3% (b) of Cl-Naph; P3HT/**Bis-PDI-T-EG** with 0% (c) and 8% (d) of Cl-Naph; P3HT/**Bis-PDI-T-di-EG** with 0% (e) and 1.75% (f) of Cl-Naph. The electron mobilities (μ_e) are listed in Table 3 in the text.

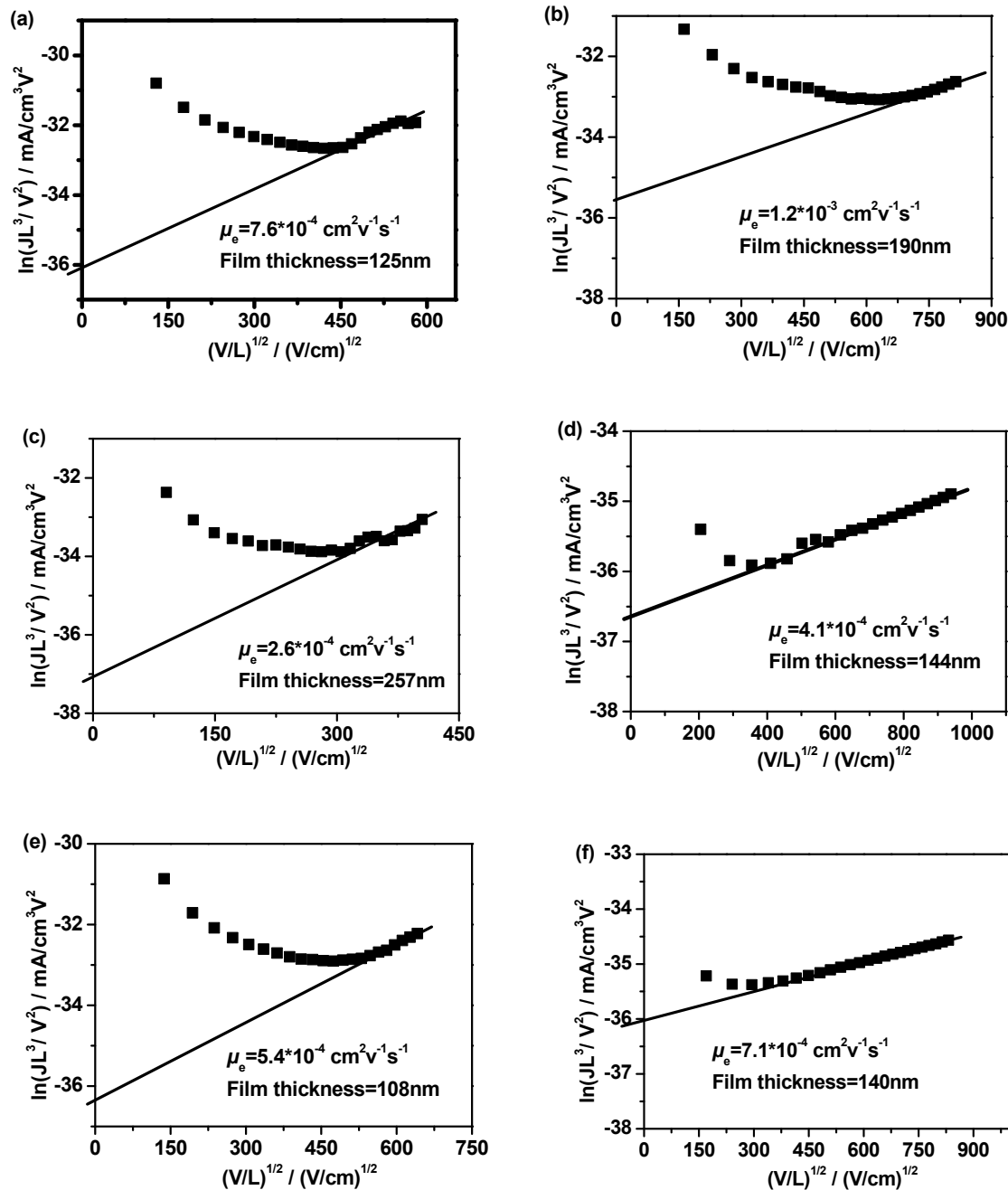
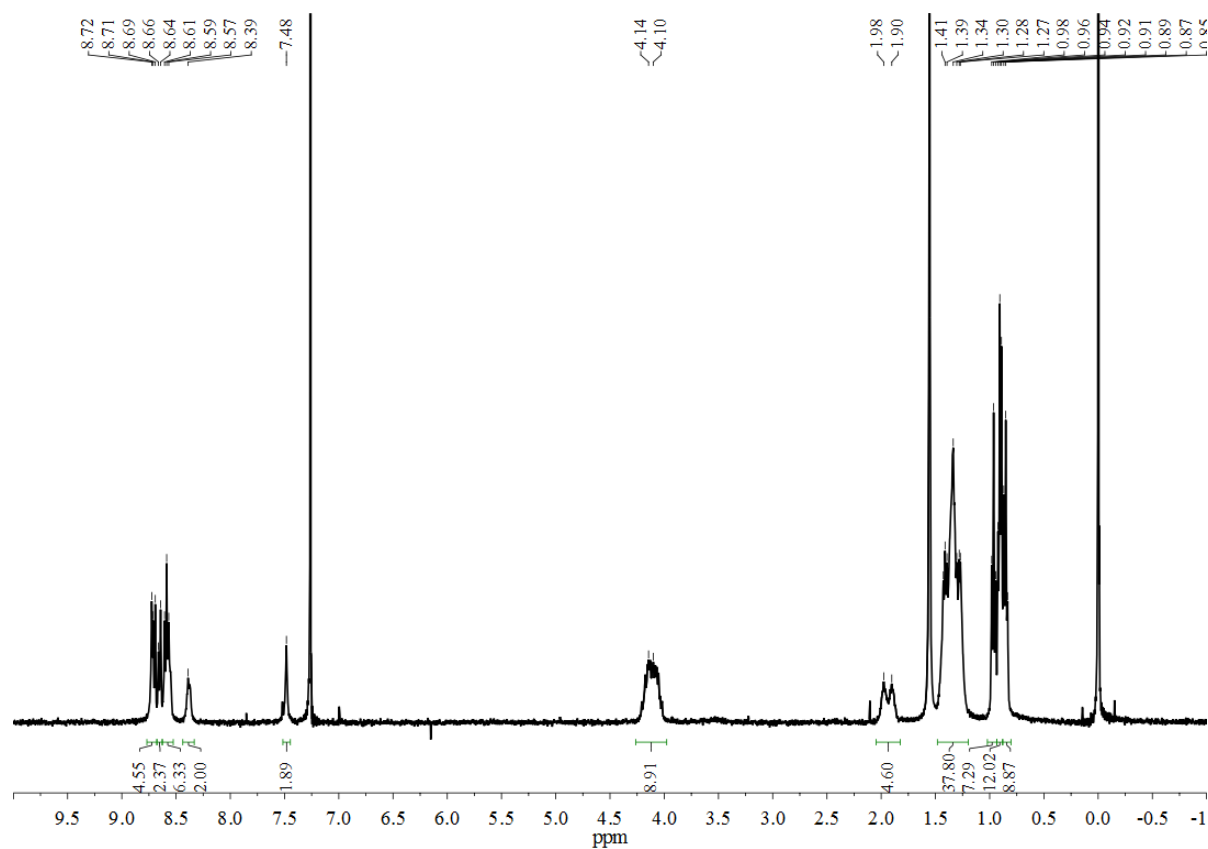
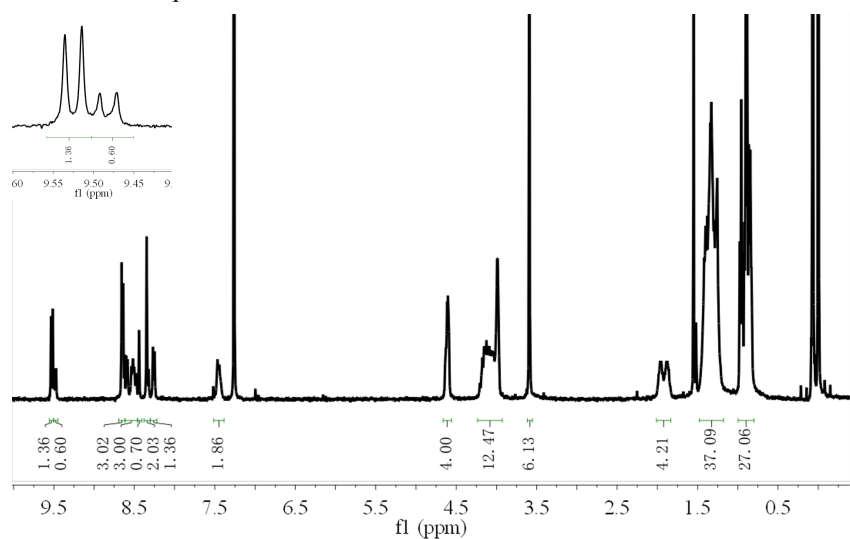


Figure S10. The ^1H NMR and ^{13}C NMR spectra of **Bis-PDI-T**, **Bis-PDI-T-EG** and **Bis-PDI-T-di-EG**.

The ^1H NMR spectrum of **Bis-PDI-T**

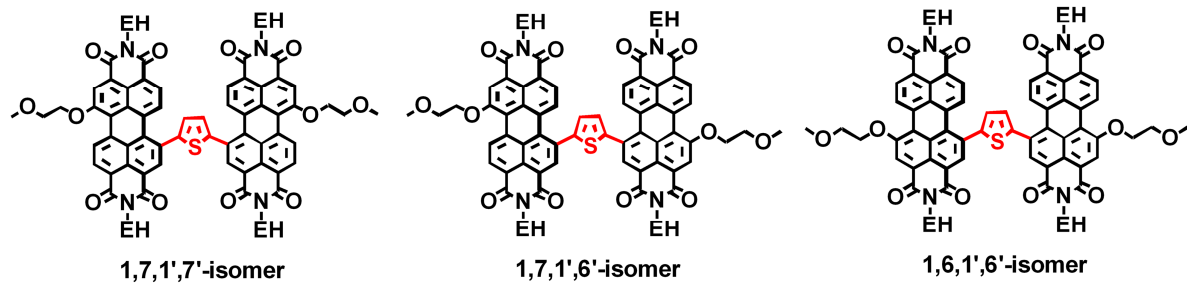


The ^1H NMR spectra of **Bis-PDI-T-EG**

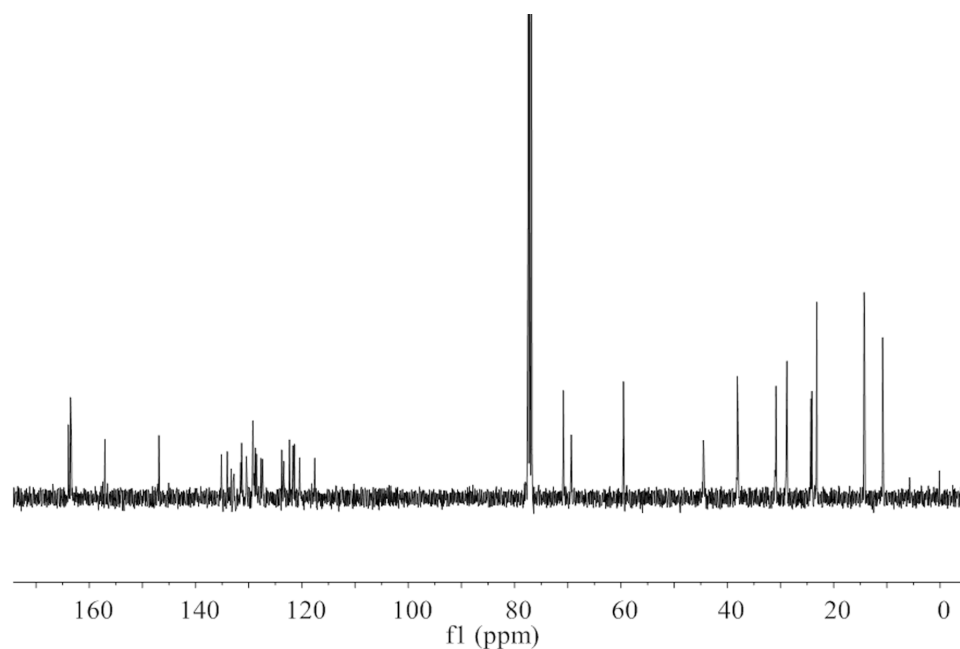


We noted that product **1** (**Bis-PDI-T-EG**) is a mixture of 1,7,1',7'-, 1,7,1',6'-, and 1,6,1',6'-regioisomers. The percentage of the 1,6-isomeric structure including that in 1,7,1',6'- and 1,6,1',6'-isomers is ~30% ($0.6/(1.36+0.60)=30.6\%$) estimated from the intergrals of the splitting peaks at about 9.5 ppm in the $^1\text{H-NMR}$ spectrum.

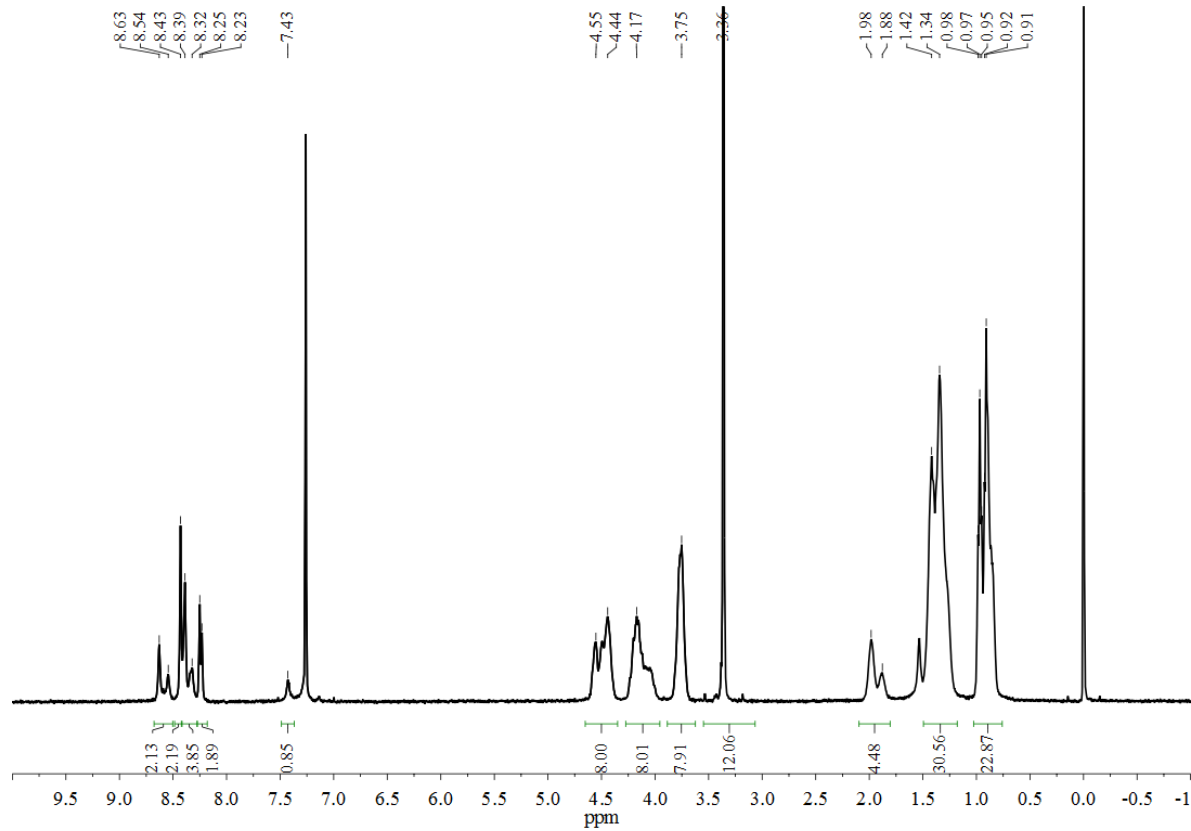
Bis-PDI-T-EG



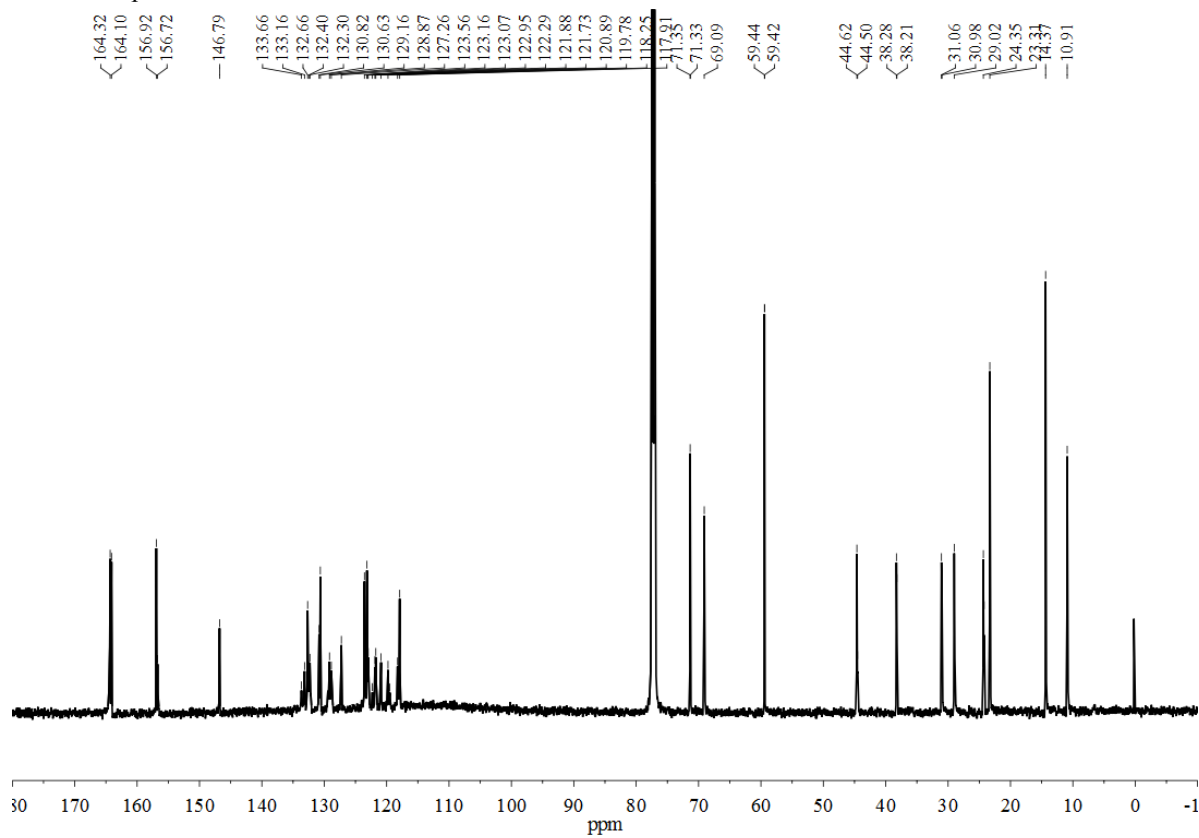
The ^{13}C NMR spectra of **Bis-PDI-T-EG**.



¹H NMR spectrum of Bis-PDI-T-di-EG



¹³C NMR spectrum of Bis-PDI-T-di-EG



4. Supporting tables

Table 1. Photovoltaic properties of **Dimeric PDI** based OSCs using different A /D ratio.

Dimeric PDI	Ratio (A/D)	Cl-Naph (% v/v)	V _{oc} (V)	J _{sc} (mA/cm ²)	FF (%)	PCE (%)
Bis-PDI-T	3:2	3	0.35	1.60	43.2	0.24
Bis-PDI-T	1:1	3	0.43	2.01	47.2	0.41
Bis-PDI-T	2:3	3	0.43	1.65	49.1	0.35
Bis-PDI-T-EG	3:2	4	0.63	2.31	39.0	0.57
Bis-PDI-T-EG	1:1	4	0.63	2.46	41.6	0.63
Bis-PDI-T-EG	2:3	4	0.63	2.02	45.8	0.58
Bis-PDI-T-di-EG	3:2	2	0.66	3.89	51.9	1.33
Bis-PDI-T-di-EG	1:1	2	0.67	3.97	55.7	1.48
Bis-PDI-T-di-EG	2:3	2	0.68	3.24	58.5	1.29

References

1. M. J. Frisch, G. W. Trucks, H. B. Schlegel, G. E. Scuseria, M. A. Robb, J. R. Cheeseman, G. Scalmani, V. Barone, B. Mennucci, G. A. Petersson, H. Nakatsuji, M. Caricato, X. Li, H. P. Hratchian, A. F. Izmaylov, J. Bloino, G. Zheng, J. L. Sonnenberg, M. Hada, M. Ehara, K. Toyota, R. Fukuda, J. Hasegawa, M. Ishida, T. Nakajima, Y. Honda, O. Kitao, H. Nakai, T. Vreven, J. A. Montgomery, Jr., J. E. Peralta, F. Ogliaro, M. Bearpark, J. J. Heyd, E. Brothers, K. N. Kudin, V. N. Staroverov, R. Kobayashi, J. Normand, K. Raghavachari, A. Rendell, J. C. Burant, S. S. Iyengar, J. Tomasi, M. Cossi, N. Rega, J. M. Millam, M. Klene, J. E. Knox, J. B. Cross, V. Bakken, C. Adamo, J. Jaramillo, R. Gomperts, R. E. Stratmann, O. Yazyev, A. J. Austin, R. Cammi, C. Pomelli, J. W. Ochterski, R. L. Martin, K. Morokuma, V. G. Zakrzewski, G. A. Voth, P. Salvador, J. J. Dannenberg, S. Dapprich, A. D. Daniels, O. Farkas, J. B. Foresman, J. V. Ortiz, J. Cioslowski, and D. J. Fox, Gaussian 09, Revision A.02, Gaussian, Inc., Wallingford CT, 2009.
2. (a) C. T. Lee, W. T. Yang, R. G. Parr, *Phys. Rev. B* **1988**, *37*, 785-789; (b) A. D. Becke, *J. Chem. Phys.* **1993**, *98*, 5648-5652.
3. R. Krishnan, J. S. Binkley, R. Seeger, J. A. Pople, *J. Chem. Phys.* **1980**, *72*, 650-654.
4. (a) G. G. Malliaras, J. R. Salem, P. J. Brock, C. Scott, *Phys. Rev. B*, **1998**, *58*, 13411; (b) T. Y. Chu, O. K. Song, *Appl. Phys. Lett.*, **2007**, *90*, 203512; (c) Z. A. Tan, W. Q. Zhang, Z. G. Zhang, D. P. Qian, Y. Huang , J. H. Hou, Y. F. Li, *Adv. Mater.*, **2012**, *24*, 1476-1481.
5. P. Rajasingh, R. Cohen, E. Shirman, L. J. W. Shimon, B. Rybtchinski, *J. Org. Chem.*, 2007, **72**, 5973-5979.
6. Zhang, X.; Pang, S. F.; Zhang, Z. G.; Ding, X. L.; Zhang, S. L.; He, S. G.; Zhan, C. L. *Tetrahedron Lett.* 2012, *53*, 1094–1097.
7. Y. G. Zhen, H. L. Qian, J. F. Xiang, J. Q. Qu, Z. H. Wang, *Org. Lett.*, 2009, **11**, 3084–3087.